Isothermal flame balls: Effect of autocatalyst decay

Éva Jakab,[1] Dezső Horváth,[1,*] John H. Merkin,[2] Stephen K. Scott,[3] Péter L. Simon,[3] and Ágota Tóth[1]
[1]*Department of Physical Chemistry, University of Szeged, P.O. Box 105, Szeged H-6701, Hungary*
[2]*Department of Applied Mathematics, University of Leeds, Leeds LS2 9JT, United Kingdom*
[3]*Department of Chemistry, University of Leeds, Leeds LS2 9JT, United Kingdom*
(Received 12 May 2003; published 19 September 2003)

The steady, spherically symmetric solutions to the reaction-diffusion equations based on a simple autocatalytic reaction followed by the decay of the autocatalyst are considered. Three parameters—the orders with respect to the autocatalyst in the autocatalysis p and in the decay q and the rate of decay of the autocatalyst relative to its autocatalytic production K—determine the steady concentration profiles. Numerical integrations for a fixed value of the order of the autocatalyst show that the concentration profiles have different forms depending on whether $q<p$ or $q\geqslant p$. In the former case, there is a critical decay rate K_{crit} for solutions to exist, with multiple solutions for $K<K_{crit}$. In the latter case, there is a single solution for each value of K. This difference in the nature of the solution is confirmed by an analysis for p large. The temporal stability of the isothermal flame balls is examined, with temporally stable solutions being possible, provided that the ratio of the diffusion coefficient of the autocatalyst to that of the reactant is sufficiently small. The change in stability appears only when there are multiple solutions and is through a subcritical Hopf bifurcation.

DOI: 10.1103/PhysRevE.68.036210 PACS number(s): 89.75.Kd, 47.54.+r, 02.30.Mv, 82.33.Vx

I. INTRODUCTION

In a previous paper [1] we considered the steady, spherically symmetric solutions on an infinite domain to a system of reaction-diffusion equations based on the single autocatalytic reaction

$$A+p\,B\rightarrow(p+1)B, \quad \text{with rate} \quad k_1ab^p, \tag{1}$$

where $p\geqslant 1$, and a and b are the concentrations of reactant A and autocatalyst B. We showed that a transformation of variables reduced the problem to a single equation in which p, the order of the autocatalysis, was the only parameter. This equation has solutions satisfying the required boundary conditions only if $p>5$. For $1\leqslant p<5$, all (positive) solutions have compact support, i.e., they are zero out of a bounded domain. We examined the nature of the solution both as $p\rightarrow 5^+$ and when p was large.

A further consideration of the time-dependent problem set up in Ref. [1] showed that these solutions were temporally unstable to perturbations in the radial direction. Our study was motivated, in part, by the classic problem of ''flame balls,'' or steady, radially symmetric solutions of the reaction-diffusion-conduction equations for premixed laminar flames first identified by Zel'dovich [2]. In this context, these solutions are also unstable in the adiabatic limit, though they can become stable if there is a (small) heat loss [3]. The analogy between the feedback through the temperature in combustion systems and through the autocatalyst in isothermal systems of the type given by Eq. (1) has previously been recognized. It has been shown [4] that a simple cubic autocatalysis with appropriate difference in diffusivities can lead to cellular fronts similar to those observed in premixed flames with small Lewis numbers [5]. We would like to explore to what extent the analogy between premixed combustion and isothermal autocatalytic systems can be drawn. Spherical flames may be stabilized by radiative heat loss, which then suggests an extension to our kinetic scheme to include the additional decay step

$$B\rightarrow C, \quad \text{with rate} \quad k_2b^q \quad (q\geqslant 1), \tag{2}$$

whereby the autocatalyst decays to an inert product C as a kinetic mimic of heat loss. In studies of flame balls, radiation introduces a term with T^n with $n=2-4$ in the energy balance [3,6]; we therefore investigate the behavior of our system for various values of q. The traveling front structures that the reaction scheme in Eqs. (1) and (2) can support have been examined in Refs. [7–10], where it was seen that the additional decay step can make qualitative differences in the behavior of the solution. It can totally inhibit traveling front formation as well as making substantial changes to the traveling front profiles that would otherwise form.

Here we consider the steady, spherically symmetric solutions to the reaction-diffusion equations with reactions in Eqs. (1) and (2) as the kinetics. We are unable, as in Ref. [1], to reduce the problem to a single equation, but we can make some simplifications to reduce the number of parameters to p and q (orders of the autocatalysis and decay) and a further parameter K which represents the rate of decay of B relative to its autocatalytic production. Numerical integrations for a fixed value of p show that the solution has a different form depending on whether $q<p$ or $q\geqslant p$. In the former case, there is a critical value K_{crit} of K for solutions to exist, with multiple solutions for $K<K_{crit}$. In the latter case, there is a single solution for each value of K. This difference in the nature of the solution is confirmed by an analysis for p large. We also examine the temporal stability of the solutions, finding stabilization, provided that D, the ratio of the diffusion coefficient of B to that of A, is sufficiently small. This change

*Email address: horvathd@chem.u-szeged.hu

in stability appears only when there are multiple solutions and is through a subcritical Hopf bifurcation in the cases studied here.

II. MODEL SYSTEM

The equations governing the reaction and diffusion of the two reactants A and B are (see Refs. [8,11–13], for example)

$$\frac{\partial a}{\partial t}=D_A\nabla^2 a-k_1 ab^p, \quad \frac{\partial b}{\partial t}=D_B\nabla^2 b+k_1 ab^p-k_2 b^q, \tag{3}$$

where D_A and D_B are the diffusion coefficients of A and B, respectively, subject to the boundary conditions

$$a\to a_0, \quad b\to 0 \quad \text{as} \quad |\mathbf{x}|\to\infty, \tag{4}$$

representing only reactant A sufficiently far from the reaction zone and initial condition that

$$a=a_0, \quad b=0 \quad \text{at} \quad t=0 \tag{5}$$

for all $\mathbf{x}$, i.e., a homogeneous distribution of pure A apart from some local region, centered on the origin, where there is some input of B to start a reaction. We make Eq. (3) dimensionless using the reaction time $(k_1 a_0^p)^{-1}$ and a length scale based on this and D_A, by putting

$$a=a_0\,\overline{a}, \quad b=a_0\,\overline{b}, \quad \overline{t}=(k_1 a_0^p)t, \quad \overline{\mathbf{x}}=\mathbf{x}\left(\frac{k_1 a_0^p}{D_A}\right)^{1/2}. \tag{6}$$

This leads to the dimensionless equations (on dropping the bars for convenience)

$$\frac{\partial a}{\partial t}=\nabla^2 a-ab^p, \quad \frac{\partial b}{\partial t}=D\nabla^2 b+ab^p-\kappa b^q, \tag{7}$$

where $D=D_B/D_A$ is the ratio of diffusion coefficients and $\kappa=k_2/(k_1 a_0^{p-q+1})$ is the decay rate of B with respect to the autocatalysis.

We are investigating spherically symmetric concentration profiles, i.e., solutions to the equations

$$\frac{\partial a}{\partial t}=\frac{\partial^2 a}{\partial r^2}+\frac{2}{r}\frac{\partial a}{\partial r}-ab^p,$$

$$\frac{\partial b}{\partial t}=D\left(\frac{\partial^2 b}{\partial r^2}+\frac{2}{r}\frac{\partial b}{\partial r}\right)+ab^p-\kappa b^q, \tag{8}$$

on $0<r<\infty$, $t>0$, where r measures the (radial) distance from the origin, subject to

$$a, b \quad \text{continuous at} \quad r=0, \quad a\to 1, b\to 0 \quad \text{as} \quad r\to\infty \quad (t>0), \tag{9}$$

$$a=1, \quad b=b_i g(r) \quad \text{at} \quad t=0 \quad (0<r<\infty),$$

where b_i is a positive constant and $g(r)$ is some smooth function, nonzero only for a finite range of r with a maximum value of unity, defining the local input of the autocatalyst to initiate the reaction. We start by considering the existence of reaction balls which are steady state solutions to Eqs. (8) and (9).

III. STEADY SOLUTIONS

We can, following the approach given in Ref. [1], scale out the ratio of diffusion coefficients, D, from the equations for the steady solutions—Eqs. (8) with vanishing time derivatives—by substituting

$$b=D^{-1}\tilde{b}, \quad \tilde{r}=D^{-p/2}r, \tag{10}$$

and leaving a unchanged. This leads to the reduced system (on omitting the tildes)

$$a''+\frac{2}{r}a'-ab^p=0, \quad b''+\frac{2}{r}b'+ab^p-K\,b^q=0 \tag{11}$$

still subject to Eq. (9), where $K=D^{p-q}\kappa$ and where primes denote differentiation with respect to r.

The steady states are then dependent only on the single parameter K, representing the relative decay rate of the autocatalyst in the new coordinate system; though we note that their temporal stability depends separately on both D and K (or κ). It is the nontrivial (i.e., $a\not\equiv 1$, $b\not\equiv 0$) solutions to Eqs. (11) subject to Eq. (9) that we now consider in detail.

A. Numerical simulations

We obtain numerical solutions of Eq. (11) that are bounded as $r\to 0$. This means that they have the form

$$a=a_0+\left(\frac{a_0 b_0^p}{6}\right)r^2+\left(\frac{a_0 b_0^{2p}+p a_0 b_0^{p-1}(Kb_0^q-a_0 b_0^p)}{120}\right)r^4 +O(r^6), \tag{12}$$

$$b=b_0-\frac{1}{6}(a_0 b_0^p-Kb_0^q)r^2 -\left(\frac{a_0 b_0^{2p}-(p a_0 b_0^{p-1}-qKb_0^{q-1})(a_0 b_0^p-Kb_0^q)}{120}\right)r^4 +O(r^6),$$

for r small resulting from the zero-concentration gradients at the origin. Here a_0 and b_0 are the central concentrations of the reactant A and autocatalyst B, respectively, to be determined in the numerical integrations.

Previously [1] (with $K=0$) we obtained the ground states or fastest decaying solutions representing the critical distribution of B, above which an outpropagating front is generated and below which the initiation collapses to the trivial state containing only reactant A. This meant looking for solutions which were $O(r^{-1})$ for r large. The situation is different with $K>0$, and the form for b which decays fastest as $r\to\infty$ needs to be considered. For $q=1$ the analytical solution is taken at the limit $r\to\infty$, for $q\neq 3$ the form of b

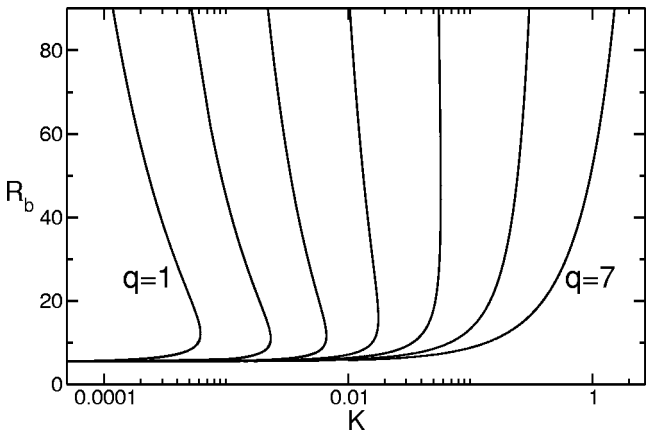

FIG. 1. Reaction radius R_b as a function of K for $p=6$ and range of values for q from $q=1$ to $q=7$.

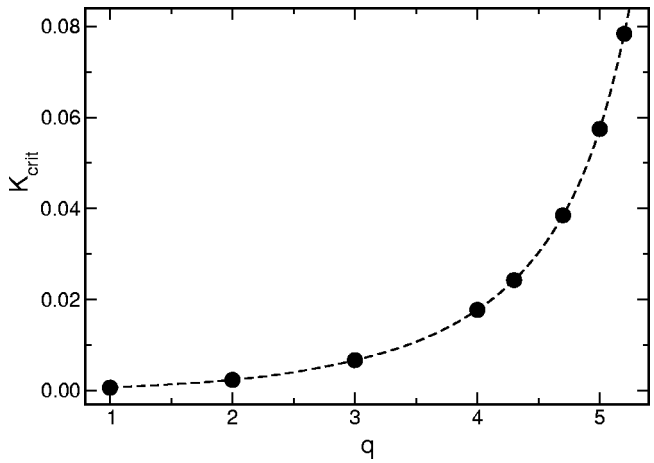

FIG. 2. Variation of K_{crit} with q for $p=6$.

$\sim O(r^{-m})$ is tested while for $q=3$, $b\sim O(r^{-1}[\ln(r)]^{-m})$ is applied for matching the exponents in the terms with leading order, resulting in

$$b\sim \frac{C_2}{r}e^{-\sqrt{K}r} \quad \text{for } q=1, \tag{13}$$

$$b\sim \frac{C_2}{r^{2/(q-1)}} \quad \text{for } 1<q<3,$$

$$b\sim \frac{C_2}{r\sqrt{\ln r}} \quad \text{for } q=3,$$

$$b\sim \frac{C_2}{r} \quad \text{for } q>3$$

for r large, taking

$$a\sim 1-\frac{C_1}{r} \tag{14}$$

in all cases with C_1 and C_2 constants that are also determined in the numerical integrations.

The solutions for small and large r given by Eqs. (12)–(14) were joined numerically using a standard shooting method for solving boundary-value problems. The solution was calculated at $r=0.001$ using Eq. (12), and this was extended numerically using the CVODE package [14]. The values of a_0 and b_0 were adjusted until the behavior given by (13) and (14) was approached at a large value of r. We found that taking values of r between 200.0 and 400.0 gave sufficient accuracy. This procedure determines the values of a_0, b_0, C_1, and C_2 for given values of K,p,q.

For the results presented below we select $p=6$, being the smallest integer where a stationary spherical solution exists for $K=0$ [1], and consider different values for q. In Fig. 1 we plot the ''reaction radius'' R_b against K, where R_b is the position at which the local autocatalytic reaction r^2ab^p achieves its maximum value. We identify two qualitatively different types of behavior. The curves for those values of q such that $q<p$ have a qualitatively similar form, in that there is a critical value K_{crit} for K. A saddle-node bifurcation occurs at $K=K_{crit}$, with no solutions for $K>K_{crit}$ and two solution branches for $K<K_{crit}$. The figures resemble those observed in flame studies where the radius is shown against the parameter representing heat loss [3,6]. All the lower branch solutions start at the same value for R_b as $K\to 0$, the value obtained in Ref. [1] for $p=6$, and the upper branch solutions appear to approach the $K=0$ axis as K decreases. The curves for values of $q\geqslant p$ $(q=6,7)$ are monotone, with R_b increasing as K is increased. A graph of K_{crit} against q, shown in Fig. 2, illustrates that K_{crit} increases very rapidly as q approaches $q=6$ (as $q\to p^-$), as perhaps could be expected.

Typical differences between the lower and upper branch concentration profiles (as identified in Fig. 1) can be seen in Fig. 3(a), where we plot a and b profiles for $p=6$, $q=1$, and $K=0.0001$. The outer boundary conditions are approached at relatively small values of r for the lower branch solutions (broken lines), whereas considerably larger values of r are required for the upper branch solutions (full lines). The values of both a_0 and b_0 are higher for the lower branch solutions which are monotone (increasing for a and decreasing for b). The upper branch profile for b has a local maximum (in this case of approximately 0.393 28 at $r=r_m\simeq 60.9$) before decreasing to zero for large r. This internal maximum is a feature of the profiles for smaller values of K and is lost at higher K, as can be seen in Fig. 3(b) where we plot the corresponding profiles for $K=0.0005$. Here the (upper branch) profile for b is monotone decreasing though there is central region where b takes almost constant values and a is almost zero. This effect is also seen in Fig. 3(a). The concentration profiles of the autocatalyst b again return the characteristics of observed temperature distributions in flame balls [15,16].

The features noted for the concentration profiles shown in Fig. 3 are brought out more clearly in Fig. 4. In Fig. 4(a) we plot b_0, the concentration of the autocatalyst B at the center, against K (again for $p=6,q=1$), the values corresponding to the upper and lower branches shown in Fig. 1 are noted on the figure. This figure shows clearly that b_0 is always greater

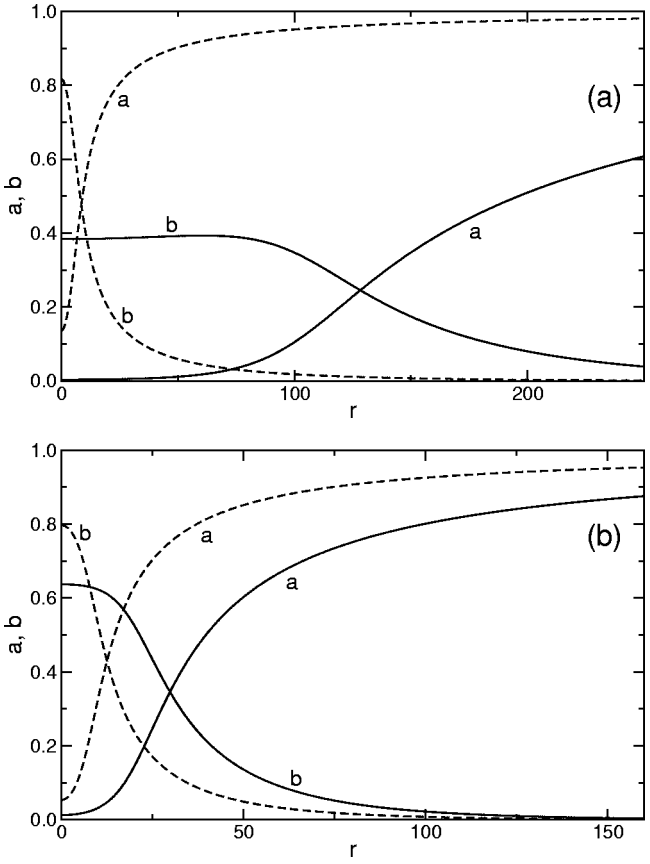

FIG. 3. Concentration profiles a and b for the upper branch (full lines) and the lower branch (broken lines) for $p=6$, $q=1$, and (a) $K=10^{-4}$ and (b) $K=5\times10^{-4}$.

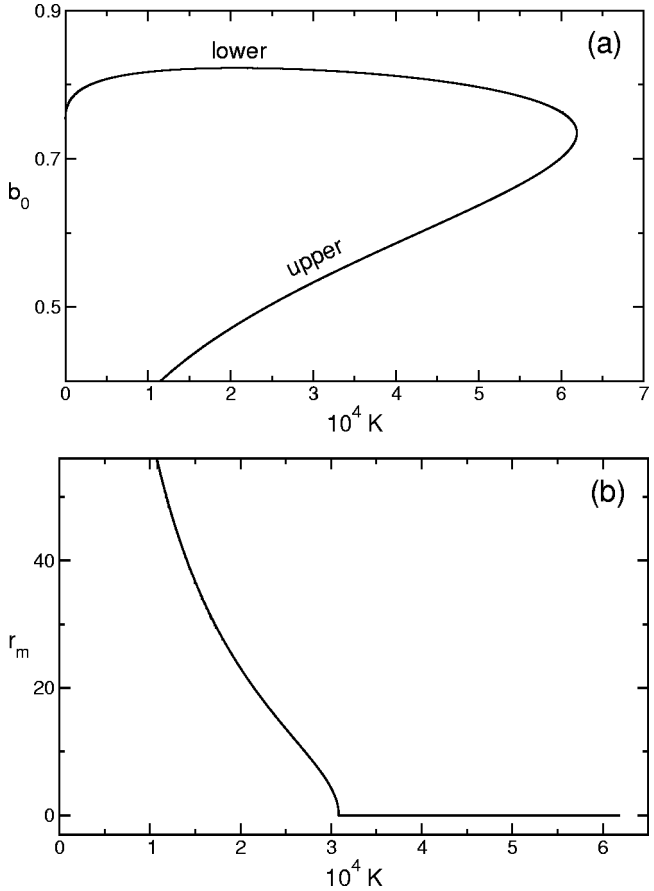

FIG. 4. (a) Variation of the concentration of B at the center ($r=0$) with K. (b) Dependence of r_m, the position where b achieves its local maximum (upper branch solutions), on K. Both graphs are for $p=6$, $q=1$.

for the lower branch solutions than for upper branch solutions. An analogous temperature difference for the upper and lower branches has led to the labeling as ''cold giant'' and ''hot dwarf,'' respectively, in flame studies [6]. Note that, for the lower branch, b_0 increases initially with K from its value for $K=0$ before decreasing to its value at the saddle-node bifurcation. In Fig. 4(b) we plot r_m, the position of the internal maximum in b for the upper branch solutions. The figure emphasizes that this effect requires K to be relatively small, i.e., $K<K_0$ ($K_0\simeq3.083\times10^{-4}$ for this case). For $K>K_0$, $r_m=0$ and b is monotone decreasing for all r.

The asymptotic solution for $p\gg1$ obtained in Ref. [1] provided useful insights into the nature of the solution when $K=0$. This limit is also a useful guide to the behavior of the solution when $K\neq0$, and it is this limit that we consider next.

B. Solution for p large

In this section we derive a relation between K and the reaction radius R_b analytically, using an asymptotic expansion for large values of p. This relation arises from a boundary-value problem, i.e., a boundary-value problem will be derived, and for a given value of K the value of R_b can be obtained by solving this problem. We concentrate on the case where $q\sim p\gg1$, and to obtain a consistent matching for this case we require that K be small, of the order $O(p^{-3})$. We then take

$$q=p\,q_0,\quad \overline{K}=\frac{K}{p^3}, \tag{15}$$

where q_0 and $\overline{K}$ are $O(1)$. In this case the structure of the solution for $K\neq0$ for p and q large is similar to that found in Ref. [1] when $K=0$. There is a relatively thin reaction region at a distance $X(p)$ of $O(p)$ from the center. Ahead of this is a thicker outer region which is dominated by diffusion. The central inert core region, seen when $K=0$, now becomes a region in which the effects of the decay reaction in Eq. (2) are significant. It is the matching of the solutions in these three regions that determines the ''reaction radius'' in terms of $\overline{K}$. The details of the calculations are given in Appendix A. Here we present the main results of the matching.

We look for a solution of Eqs. (11) by putting $r=pX(p)+\overline{r}$ and expanding

$$X(p)=X_0+X_1p^{-1}+\cdots.$$

At leading order we obtain a relation between X_1 and X_0, namely,

$$X_0^2=\frac{1}{2}e^{X_1/X_0} \tag{16}$$

(see Appendix A for further details). The description is completed and X_0 determined in the inner region, where whole of the reactant A has been consumed and in which we put

$$\overline{Y}=\frac{r-pX(p)}{X_0 p}, \quad b=1-p^{-1}(U_0+p^{-1}U_1+\cdots).$$

Here $\overline{Y}$ is a modified space variable and $U_0, U_1, \ldots$ represent the concentration of B. Solving the resulting boundary-value problem

$$U_0''+\frac{2}{1+\overline{Y}}U_0'+\overline{K}X_0^2 e^{-q_0 U_0}=0, \tag{17}$$

$$U_0(0)=U_0'(0)=\frac{X_1}{X_0}, \quad U_0 \text{ bounded at } \quad \overline{Y}=-1 \tag{18}$$

together with Eq. (16), gives the relation between $\overline{K}$ and X_0. We note that, if $\overline{K}=0$, then $U_0\equiv 0$, $X_1=0$, and Eq. (16) gives the value $X_0=1/\sqrt{2}$ found in Ref. [1]. For $\overline{K}\neq 0$, Eqs. (17) and (18) have to be solved numerically to determine X_1/X_0, which can then be used in Eq. (16) to determine how X_0 varies with $\overline{K}$. Note that X_0 gives the location of the autocatalytic reaction (to leading order) and is effectively the reaction radius R_b used in Fig. 1.

The results are shown in Fig. 5 where we plot X_1/X_0 against $\overline{K}$ for a range of q_0, which is essentially $\ln(R_b)$ plotted against K/p^3. The important point to note from the figure is that there is a critical value $\overline{K}_{crit}$ of $\overline{K}$ for $q_0<1$ [Fig. 5(a)] and no such critical value for $q_0\geqslant 1$. This is illustrated in Fig. 5(b) where we contrast results for $q_0=0.95$ with those for $q_0=1$, 1.05. The values of $\overline{K}_{crit}$ are relatively large and increase considerably as $q_0\to 1$ from below. This can be seen in Fig. 5(a) and more clearly in Table I, where we give $\overline{K}_{crit}$ for increasing values of q_0. For $p=6$ and $q_0=5/6$ (corresponding to the largest value of q plotted in Fig. 2), we obtain $K_{crit}=0.229$ from the $p\gg 1$ solution. This is somewhat of an overestimate of the value $K_{crit}=0.057\,469\,7$ obtained from the numerical solutions, though good agreement at this relatively low value of p could not really be expected. It is shown directly in Appendix B that having $q_0<1$ (i.e., having $q<p$) is necessary for multiple solutions.

A relatively straightforward regular expansion in $\overline{K}$ for the lower branch solutions gives

$$X=\frac{1}{\sqrt{2}}\left(1+\frac{\overline{K}}{12}+O(\overline{K}^2)\right)$$

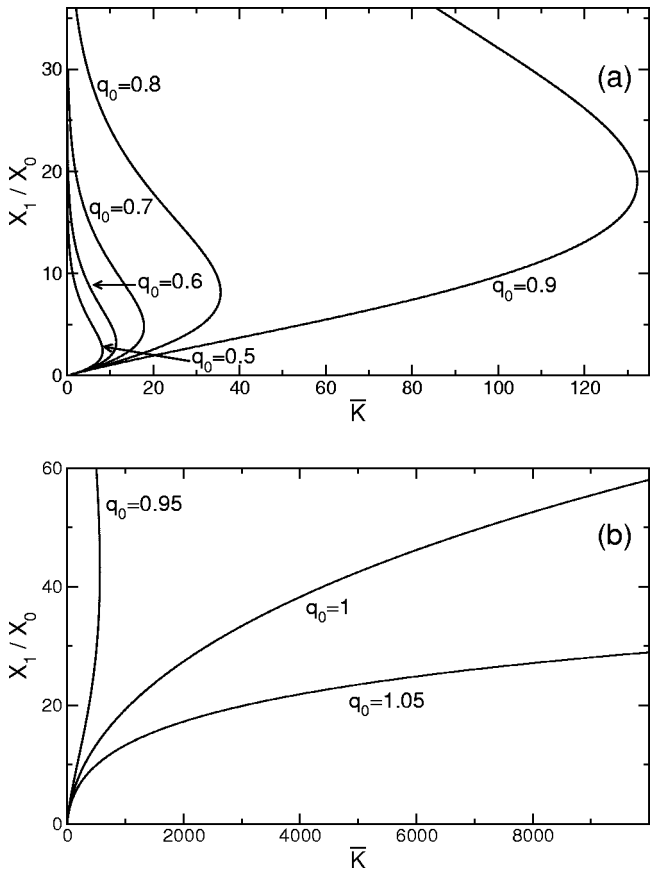

FIG. 5. Plots of X_1/X_0 against $\overline{K}$ obtained from the numerical solution of Eqs. (17) and (18) for the asymptotic expansion for p large. The position of the ''reaction radius'' is given by X_0, where $X_0=\exp(X_1/2X_0)/\sqrt{2}$; (a) $q_0=0.5,0.6,0.7,0.8,0.9$ and (b) $q_0=0.95,1,1.05$ to show that $q_0<1$ is necessary for the existence of a critical point.

$$\text{or} \quad R_b=\frac{p}{\sqrt{2}}\left(1+\frac{K}{12p^3}+\cdots\right) \quad \text{for } \overline{K} \text{ small.} \tag{19}$$

This expansion is independent of q_0 up to $O(\overline{K})$, and so all the lower branch solutions leave the $\overline{K}=0$ axis (at X_0

TABLE I. Values of $\overline{K}_{crit}$ for different q_0 obtained from Eq. (A14) for the asymptotic expansion for p large.

q_0	$\overline{K}_{crit}$
0.2000	4.4149
0.5000	8.2407
0.6000	11.3957
0.7000	17.8472
0.8000	35.6098
0.8333	49.5666
0.9000	132.2332
0.9500	563.5950

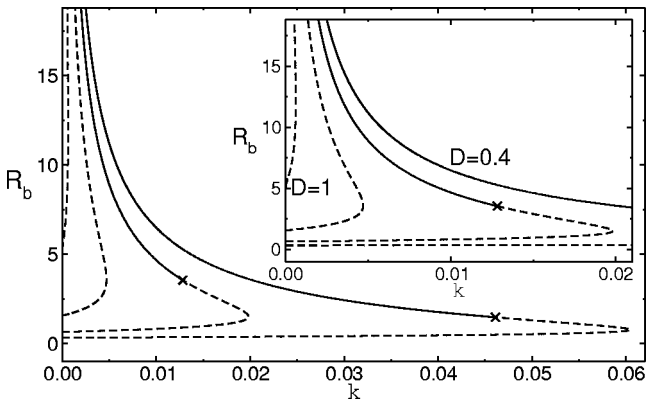

FIG. 6. Graph of the reaction radius R_b as a function of κ for $p=6, q=1$ and range of values for $D=1,2/3,0.5,0.4$. The broken lines correspond to unstable and the full lines to stable solutions.

$=1/\sqrt{2}$) with the same slope. This can be clearly seen in Fig. 5(a) and is also a feature of the results shown in Fig. 1.

IV. STABILITY

In our previous study [1] the steady states that we obtained were temporally unstable. They could be regarded as giving initial conditions dividing cases where propagating reaction-diffusion fronts formed from those where propagation failed and the system returned to its original unreacted state. The effect of including the decay of the autocatalyst in the reaction scheme, Eqs. (1) and (2), is to change the temporal stability and allow stable, time-independent states to form. We find that these stable states arise only on the upper branch solutions (as identified in Fig. 1), suggesting that we require higher order for the autocatalyst than for the order of the removal ($q<p$) for stable states.

To investigate the stability of the reaction balls—nontrivial solutions to Eqs. (8)—we have to treat D and κ separately [transformation (10) is appropriate only for the steady states]. We concentrate on the specific case $p=6$, $q=1$, though similar behavior has been seen for other values of q. In Fig. 6 we plot R_b against κ for a range of D. In the figure the broken lines correspond to unstable and the full lines to stable solutions. Figure 6 shows that a value of $D<1$ is necessary to have a stable state with the onset of stability occurring between $D=1/2$ and $D=2/3$.

If we examine the dominant eigenvalues arising from the linear stability analysis of the discrete system in more detail, we find that the lower branch solutions are all unstable (saddle points with real eigenvalues of opposite sign). The turning points correspond to saddle-node bifurcations (as would be expected), with the upper branch solution changing to an unstable node (positive real eigenvalues). For D sufficiently small, there are further changes, first to an unstable focus and finally to a stable focus (complex eigenvalues with the real part changing sign). Thus we can identify the change in stability as being through a Hopf bifurcation. In Fig. 7 we show how the values of $K(=D^{p-q}\kappa$, here $D^5\kappa)$, as used in the steady state solutions, at which the Hopf bifurcation occurs (on the upper branch) varies with D. In this plot the

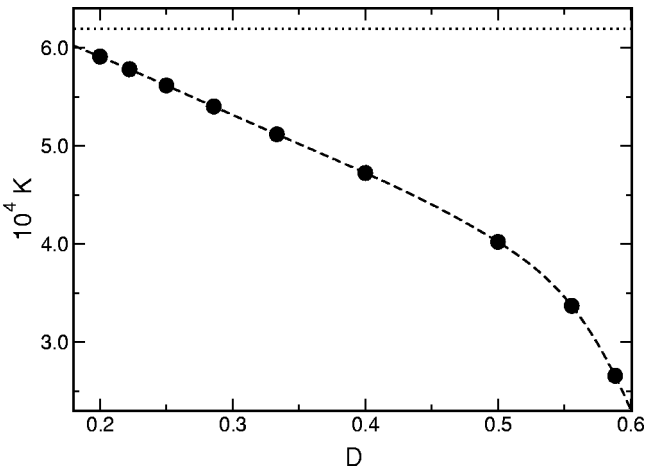

FIG. 7. Location of the Hopf bifurcation (on the upper branch solutions) for a range of D, with $p=6, q=1$. Also shown with dotted line is the location of the saddle-node bifurcation.

saddle-node bifurcation occurs at the same value of K (here at $K=6.190\,25\times10^{-4}$). The increase in the domain of stability with decreasing D is in accordance with the similar effect obtained for decreasing Lewis number for flame balls in combustion systems [3].

We integrated initial-value problem (8) numerically starting with initial profiles for a and b calculated from the shooting method used to determine the steady states. We used the same grid size that was used for the calculation of the eigenvalues. We considered a value for κ just on the unstable side of the Hopf bifurcation. The (small) errors introduced through the numerical integration of the time-dependent equations caused the system to move away from the steady state, very slowly at first, and to perform a series of relatively long-lived oscillations of slowly increasing amplitude before finally it collapsed to the state containing a homogeneous distribution of reactant A, i.e, the trivial solution of Eq. (8). The nature of these oscillations is shown in Fig. 8(a) with a

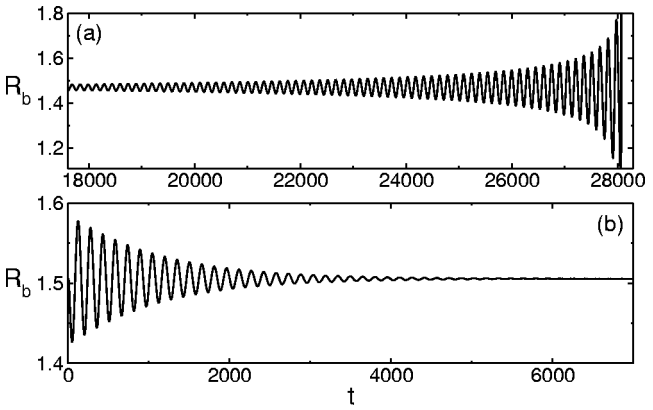

FIG. 8. Temporal evolution of the radius R_b obtained from the numerical integration of the initial-value problem (8) for $D=0.4$ and (a) $\kappa=0.046\,299\,1$, showing the oscillatory growth of the solution on the unstable side of the Hopf bifurcation, (b) $\kappa=0.045\,508$, showing the solution decaying to the steady state on the stable side of the Hopf bifurcation.

plot of R_b against t for a time period after the oscillations had become large enough to be seen graphically. For this figure, we took $\kappa = 0.046\,299\,1$, $D = 0.4$. We then changed the value of κ slightly to a value just on the stable side of the Hopf bifurcation and started the numerical integration with the previous profiles for a and b. Here the system relaxed back to the steady state appropriate for the new value of κ. This is illustrated in Fig. 8(b), for $\kappa = 0.045\,508$, still with $D = 0.4$. From the temporal evolutions we were able to estimate the eigenvalues associated with it, and these were found to be in good agreement with those calculated from the linear stability analysis.

V. CONCLUSIONS

We have shown that reaction balls—the steady, spherically symmetric solutions to the reaction-diffusion equations based on the autocatalytic reaction (1) coupled with the decay step (2)—depend only on the parameter K, representing the rate of decay of the autocatalyst relative to its production, as well as p and q, the orders of the autocatalysis and decay steps, respectively. The diffusion coefficients of the reactant and autocatalyst can be scaled out of the steady problem. Our results have shown that there are two types of steady states. In one, there is, for given values of p and q, a single solution for each value of K. In the other type of solution, there is a critical value K_{crit} of K with two solutions for $K < K_{crit}$ and no solutions for $K > K_{crit}$. Our numerical integrations show that the condition $q < p$ is required for multiple solutions, the solutions are monotone in K for $q \geqslant p$. We were also able to show that having $q < p$ is necessary and sufficient for multiple solutions in the large p limit. Both these conclusions strongly suggest that the condition $q < p$ is required in general for multiple solutions.

Further evidence for the distinct difference in the nature of the solution for $q < p$ and $q \geqslant p$ is provided by the traveling fronts that can form as large time solutions to reaction-diffusion equations based on Eqs. (1) and (2). General values of p and q were considered in Ref. [10], where it was deduced that, when $q > p$, there is no restriction on K for wave formation (though there is a threshold input of B for $p > 3$). When $q = p$, traveling waves can form only if $K < 1$. Specific examples of these two cases treated in Refs. [7–9] show that the solutions, when they exist, are single valued in K. When $q < p$ there is a critical value of K for the existence of waves with solutions being multivalued for values of K less than this [8].

When we considered the corresponding time-dependent problem, we noted that D, the ratio of the diffusion coefficients of autocatalyst and reactant, cannot be scaled out of the problem and that the temporal stability depended on this parameter as well. For values of D sufficiently small, a change in stability was seen to arise through a Hopf bifurcation. Our numerical study suggests that having $D < 1$ is a necessary condition but is not sufficient in general. This change in stability occurred only when there were multiple solutions (on the upper branches in Fig. 1). This suggests that having $q < p$ was also a necessary condition for stable solutions. The stability of the upper branch resembles that of flame balls with far field heat losses [3]: the stable region appears at small K and it grows towards the saddle-node bifurcation at K_{crit} on decreasing D or the corresponding Lewis number in flames. This implies that the decay of the autocatalyst outside the reaction radius—defined as the position at which the local autocatalysis achieves its maximum value—is not negligible. In all the cases we considered the Hopf bifurcation was subcritical since we were unable to find any spatially bounded, oscillatory solutions, though we did see the system undergoing a large number of oscillations before approaching the homogeneous unreacted state. Our numerical search was not exhaustive, since we were interested here in showing the possible existence of stable stationary concentration profiles. At this point we are unable to say whether there are parameter values for which the Hopf bifurcation is supercritical and bounded oscillatory profiles exist. In the context of the non-isothermal flame with heat losses [3], Buckmaster *et al.* concluded that there was no (simple) Hopf bifurcation, although they were unable to exclude the possibility of a degenerate Hopf point, and they found no stable periodic solutions in their numerical computations.

In this work we have shown the possibility of existence of stable spherical reaction fronts in isothermal autocatalytic systems with autocatalyst decay. It is a further example of analogy with pre-mixed flames in combustion studies; although experimental realization of the phenomenon may seem more difficult than that of cellular fronts [17] as a result of the high order with respect to the autocatalyst required to maintain sufficient feedback.

ACKNOWLEDGMENTS

This work was supported by the British Council and the Hungarian Scholarship Board (Ministry of Education) under their Joint Academic Research Program, the Hungarian Scientific Research Fund (OTKA Grant No. F031728), and by the ESF Scientific program REACTOR.

APPENDIX A

In this section we derive expression (16) and boundary-value problem (17,18) from Eq. (11). We start our solution in the outer diffusive region. Here we put, following [1],

$$r = pX(p) + \bar{r}, \quad \zeta = \frac{\bar{r}}{p},$$

where $X(p)$ is the location of the autocatalytic reaction in Eq. (1) and is to be determined. In this region $b < 1$ and both reaction terms are negligible for p large. We look for a solution in this region by expanding

$$X(p) = X_0 + X_1 p^{-1} + \cdots, \tag{A1}$$

$$a(\zeta;p) = a_0(\zeta) + a_1(\zeta) p^{-1} + \cdots,$$

$$b(\zeta;p) = b_0(\zeta) + b_1(\zeta) p^{-1} + \cdots.$$

We find that

$$a_0=\frac{\zeta}{X_0+\zeta},\quad a_1=-\frac{X_1\zeta}{(X_0+\zeta)^2},\tag{A2}$$

$$b_0=\frac{X_0}{X_0+\zeta},\quad b_1=-\frac{X_0X_1}{(X_0+\zeta)^2}.$$

Note that the a_i and b_i have been chosen to satisfy the outer boundary conditions with a_0 small and $b_0\simeq 1$ for ζ small, anticipating the matching with the reaction zone, which is what we now consider.

For the reaction region we leave $\overline{r}$ unscaled and put

$$a=Ap^{-1},\quad b=1-Bp^{-1}.\tag{A3}$$

This results in the equations

$$A''+\frac{2}{p(X+\overline{r}p^{-1})}A'-A(1-Bp^{-1})^p=0,\tag{A4}$$

$$B''+\frac{2}{p(X+\overline{r}p^{-1})}B'-A(1-Bp^{-1})^p+\frac{\overline{K}}{p^2}(1-Bp^{-1})^{q_0p}=0,$$

where primes denote differentiation with respect to $\overline{r}$. From Eq. (A2), the matching conditions are

$$A\sim\frac{\overline{r}}{X_0}+\left(-\frac{\overline{r^2}}{X_0^2}-\frac{X_1\overline{r}}{X_0^2}\right)p^{-1}+\cdots,\tag{A5}$$

$$B\sim\frac{\overline{r}}{X_0}+\frac{X_1}{X_0}+\left(-\frac{\overline{r^2}}{X_0^2}-\frac{2X_1\overline{r}}{X_0^2}\right)p^{-1}+\cdots$$

as $\overline{r}\to\infty$.

We look for a solution of equations (A4) by expanding

$$A(\overline{r};p)=A_0(\overline{r})+A_1(\overline{r})p^{-1}+\cdots,$$

$$B(\overline{r};p)=B_0(\overline{r})+B_1(\overline{r})p^{-1}+\cdots.\tag{A6}$$

At leading order we find

$$A_0''-A_0e^{-B_0}=0,\quad B_0''-A_0e^{-B_0}=0.\tag{A7}$$

Eliminating the reaction terms from Eqs. (A7), integrating and applying the matching conditions (A5) gives

$$A_0=B_0-\frac{X_1}{X_0}.\tag{A8}$$

We wish to apply the boundary condition $A\to 0$ as $\overline{r}\to-\infty$, i.e., whole of the reactant used up in the reaction zone, so that

$$A_0\to 0,\ B_0\to\frac{X_1}{X_0}\ \text{ as }\overline{r}\to-\infty.\tag{A9}$$

If we now use Eq. (A8) to eliminate A_0 and integrate the resulting equation once, we find on applying Eq. (A5) that $B_0\to\infty$ as $B_0'\to 1/X_0$, and that

$$B_0'^2=\frac{1}{X_0^2}-2\left(B_0-\frac{X_1}{X_0}+1\right)e^{-B_0}.\tag{A10}$$

If we now apply Eq. (A9) in Eq. (A10), we obtain

$$X_0^2=\frac{1}{2}e^{X_1/X_0}.\tag{A11}$$

To continue the solution we need to consider briefly the equations at $O(p^{-1})$. The reaction terms can be eliminated from these equations to give the single equation

$$A_1''+\frac{2}{X_0}A_0'=B_1''+\frac{2}{X_0}B_0'.$$

This equation can be integrated to give

$$A_1'=B_1'+\frac{X_1}{X_0^2}$$

on using Eq. (A8) and applying the matching conditions (A5). Now letting $A_1\to 0$ as $\overline{r}\to-\infty$, we find that

$$B_1\sim-\frac{X_1\overline{r}}{X_0^2}\ \text{ as }\overline{r}\to-\infty.\tag{A12}$$

From Eqs. (A9) and (A12) we have

$$a\to 0,\quad b\sim 1-\frac{X_1}{X_0}p^{-1}+\frac{X_1\overline{r}}{X_0^2}p^{-2}+\cdots\quad\text{as }\overline{r}\to-\infty.\tag{A13}$$

Expression (A13) suggests a further inner region in which $a\equiv 0$ and

$$b=1-Up^{-1},\quad Y=\overline{r}p^{-1},$$

where U representing the concentration of B satisfies the equation

$$U''+\frac{2}{X(p)+Y}U'+\overline{K}(1-Up^{-1})^{q_0p}=0\tag{A14}$$

(primes now denote differentiation with respect to Y). If we now look for a solution by expanding in inverse powers of p, we find that the leading order term U_0 satisfies

$$U_0''+\frac{2}{X_0+Y}U_0'+\overline{K}e^{-q_0U_0}=0,$$

$$U_0\sim\frac{X_1}{X_0}\left(1-\frac{Y}{X_0}+\cdots\right)\quad\text{as }Y\to 0^-,\tag{A15}$$

together with the condition, from Eq. (9), that U_0 is bounded as $Y\to -X_0$. To obtain the boundary-value problem in Eqs.

(17) and (18), we introduce a new modified space variable $\bar{Y}=X_0/Y$ which fixes the range of integration to $-1<\bar{Y}<0$.

APPENDIX B

In this section we show that $q_0<1$ is required for multiple solutions in Eqs. (17) and (18). Taking $U_0=(X_1/X_0)+(u/q_0)$ leads, on using Eq. (16), to the problem

$$u''+\frac{2}{1+\bar{Y}}u'+\alpha e^{-u}=0,$$

$$\text{where}\quad \alpha=\frac{\bar{K}}{2}q_0\exp\left(\frac{X_1}{X_0}(1-q_0)\right), \tag{B1}$$

$$u(0)=0,\quad u \text{ bounded at } \bar{Y}=-1. \tag{B2}$$

The problem given by Eqs. (B1) and (B2) involves only the single parameter α and its solution determines $u'(0)\equiv u_0$ as a function of α. Numerical integrations show that $u_0(\alpha)<0$ and that u_0 is monotone decreasing in α, i.e., $u_0'(\alpha)<0$ for $\alpha\geqslant 0$. Now, from Eq. (A15), $X_1/X_0=-u_0(\alpha)/q_0$, so that

$$\bar{K}=\frac{2\alpha}{q_0}\exp\left[u_0(\alpha)\left(\frac{1-q_0}{q_0}\right)\right].$$

Turning points in the bifurcation diagrams (Fig. 5) correspond to points where $d\bar{K}/d\alpha=0$ for a given q_0. Now

$$\frac{d\bar{K}}{d\alpha}=\frac{2}{q_0}\left[1+\alpha u_0'(\alpha)\left(\frac{1-q_0}{q_0}\right)\right]\exp\left[u_0(\alpha)\left(\frac{1-q_0}{q_0}\right)\right]=0. \tag{B3}$$

A necessary condition for Eq. (B3) to hold is that $q_0<1$ with turning points where $-\alpha u_0'(\alpha)=q_0/(1-q_0)$. Our numerical integration suggests that $-\alpha u_0'(\alpha)$ grows without bound as α increases, so $q_0<1$ is a sufficient condition as well.

[1] É. Jakab, D. Horváth, J.H. Merkin, S.K. Scott, P.L. Simon, and Á. Tóth, Phys. Rev. E **66**, 016207 (2002).

[2] Y.B. Zel'dovich, *Theory of Combustion and Detonation of Gases* (Academy of Sciences, Moscow, 1944).

[3] J.D. Buckmaster, G. Joulin, and P.D. Ronney, Combust. Flame **84**, 411 (1991).

[4] D. Horváth, V. Petrov, S.K. Scott, and K. Showalter, J. Chem. Phys. **98**, 6332 (1993).

[5] G.I. Sivashinsky, Combust. Sci. Technol. **15**, 137 (1977).

[6] J. Buckmaster, M. Smooke, and V. Giovangigli, Combust. Flame **94**, 113 (1993).

[7] J.H. Merkin, D.J. Needham, and S.K. Scott, Proc. R. Soc. London, Ser. A **424**, 187 (1989).

[8] J.H. Merkin and D.J. Needham, Proc. R. Soc. London, Ser. A **430**, 315 (1990).

[9] J.H. Merkin and D.J. Needham, Proc. R. Soc. London, Ser. A **435**, 531 (1991).

[10] D.J. Needham and J.H. Merkin, Philos. Trans. R. Soc. London, Ser. A **337**, 261 (1991).

[11] S.K. Scott, *Chemical Chaos* (Clarendon Press, Oxford, 1991).

[12] K. Showalter, Nonlinear Sci. Today **4**, 3 (1995).

[13] P. Gray and S.K. Scott, *Chemical Oscillations and Instabilities: Non-linear Chemical Kinetics* (Clarendon Press, Oxford, 1990).

[14] S.D. Cohen and A.C. Hindmarsh, Comput. Phys. **10**, 138 (1996).

[15] M. Abid *et al.*, Combust. Flame **116**, 348 (1999).

[16] M.S. Wu, P.D. Ronney, R.O. Colantonio, and D.M. Vanzandt, Combust. Flame **116**, 387 (1999).

[17] D. Horváth and Á. Tóth, J. Chem. Phys. **108**, 1447 (1998).